

Supplementary Information

'Smart' Nickel Oxide based core-shell nanoparticles for combined chemo and photodynamic cancer therapy.

DPBF assay

A freshly prepared 1,3-diphenylisobenzofuran (DPBF) (0.08 mM) solution (0.05 mg/mL in DMSO, 100 μ L) was added into 1 mL volume containing 10 μ g/mL of NOPs and was irradiated at room temperature. The decrease in the absorbance triggered by photobleaching of DPBF was measured at 410 nm through UV-VIS spectrophotometer. Natural logarithm values of absorption of DPBF were plotted against the irradiation time and fitted by a first-order linear least-square model to get the decay rate of the photosensitized process. The $^1\text{O}_2$ quantum yield of NOPs was calculated by comparison with methylene blue ($\Phi_{\text{MB}} = 0.53$ in ethanol) using the following equation^[16].

$$\Phi_{\text{NOPs}} = \Phi_{\text{MB}} (I_{\text{NPs}} / I_{\text{MB}}).$$

Induction of oxidative stress

Lipid peroxidation levels (LPO) were measured by the thiobarbituric acid (TBA) reaction by measuring the formation of malondialdehyde (MDA), a product of membrane LPO. This method was used to measure spectrophotometrically the color produced by the reaction of TBA with MDA at 532 nm. Pre-seeded cultures were exposed to nanoparticles for 24 hours, washed twice and harvested in ice-cold phosphate buffer saline at 4 °C. Cells were then lysed and centrifuged at 15000g for 10 minutes at 4 °C. To the cell lysate 10% SDS was added (in equal amount) and samples were incubated at room temperature for 5 minutes. Then, 0.25 mL of TBA (5.2 mg/mL) was added to

the mixture and incubated at 95 °C for 45 minutes. Absorbance was measured at 532 nm by Nano Drop 2000 (Thermo Fisher Scientific).

All above experiments on HeLa cells were performed twice in triplicate.

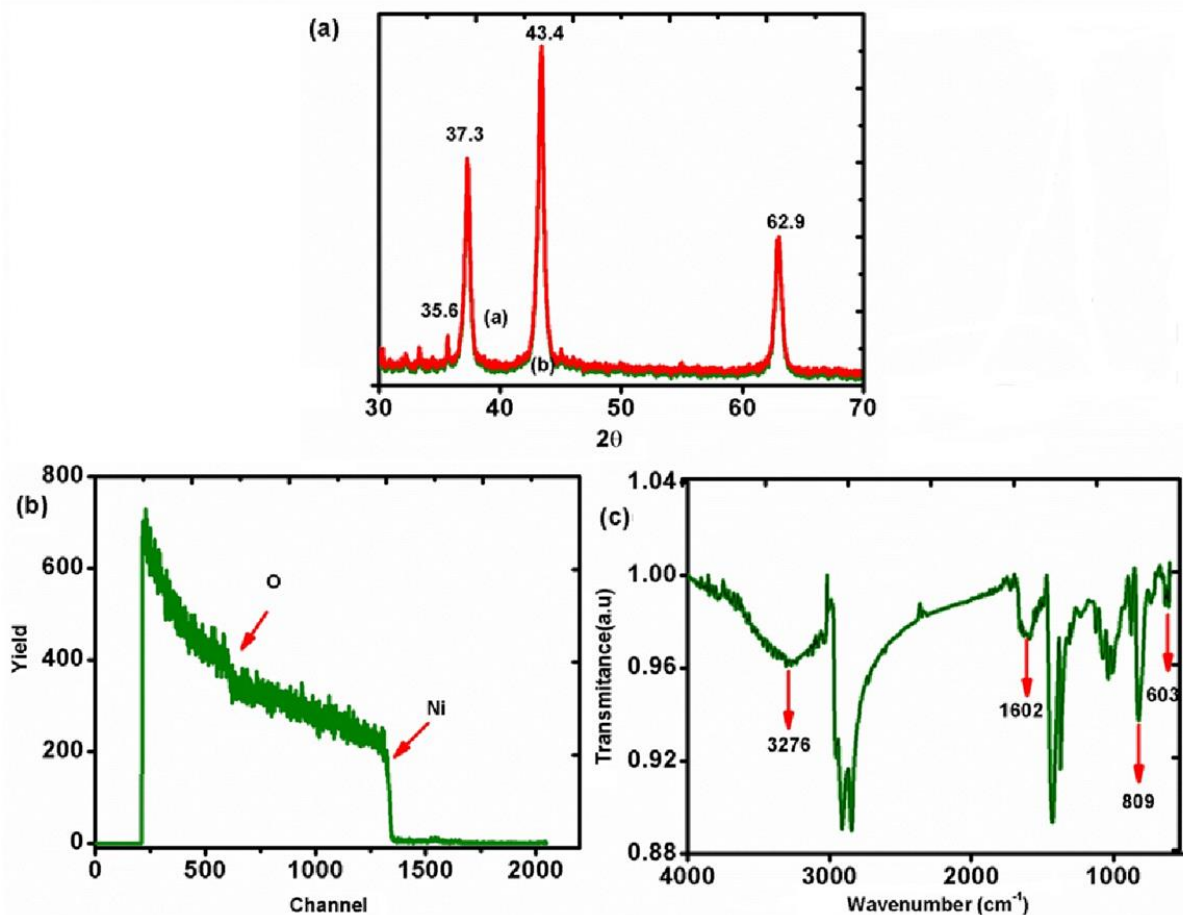


Figure S1. XRD patterns, Rutherford back-scattering and FTIR spectra of NiO nanoparticles

(a) The XRD patterns of nascent NiO with diffraction peaks at 37.3° , 43.4° and 62.9° can be assigned to face-centered cubic (fcc) nickel oxide, (111), (200) and (220) reflections consistent with NiO (JCPDS card no. 22-1189). There is no differential change in the peaks of XRD pattern obtained after 3 months (colored green indicated as b). (b) The RBS analysis gives the Ni:O ratio as 1:0.97 after data analysis with software XRUMP and SIMNRA. The 1:1 ratio of Nickel to oxygen confirms presence of NiO as already confirmed by the XRD analysis in part a. (c) FTIR spectra showed absorption band in the region of $600\text{--}700\text{ cm}^{-1}$ is assigned

to Ni–O stretching vibration mode. The broad absorption band centered at 3276 cm^{-1} is attributable to the band O–H stretching vibrations and the weak band near 1602 cm^{-1} is assigned to H–O–H bending vibrations in NiO nanoparticles.

(a).

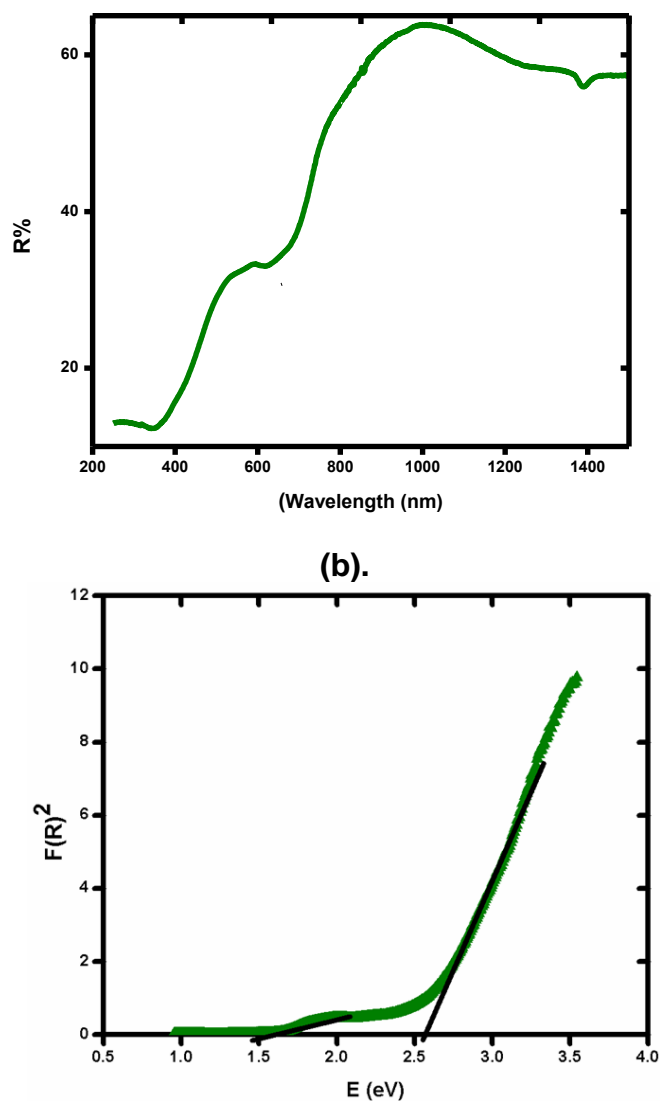


Figure S2 Diffuse reflectance spectra (DRS) and band-gap energies of NiO.

(a) DRS spectrum of NiO showed a very small peak below at 615 nm that was the absorption in visible region. While characteristic absorption edge near 1386 nm related to oxygen defects. (b) Band gap analysis of the NiO, derived by plotting the square root of the Kubelka-Munk function $F(R)^2$ vs energy in electron volts (eV). The direct band gap energies of as synthesized samples were estimated from the intercept of tangents drawn to the plots shown in Figure. Band gap analysis of the NiO was taken to test their

light response in visible region and their capability towards the photodynamic therapy. The band gap energies were found as 1.5 eV and 2.5 eV indicating low-band gap semiconductor properties of NiO.

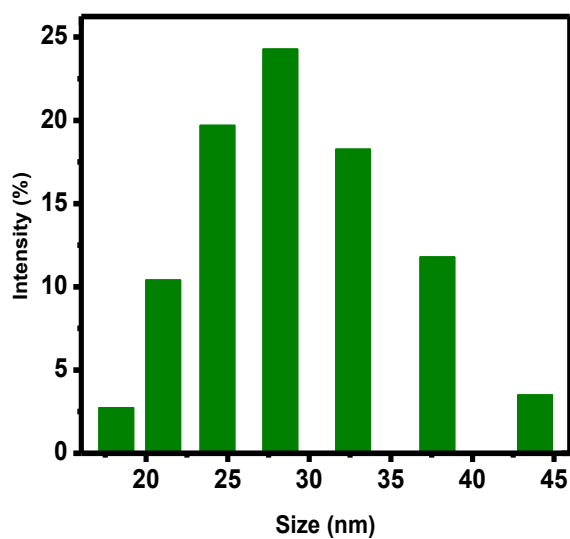


Figure S3 Average hydrodynamic diameter of surface modified nickel oxide nanoparticles.

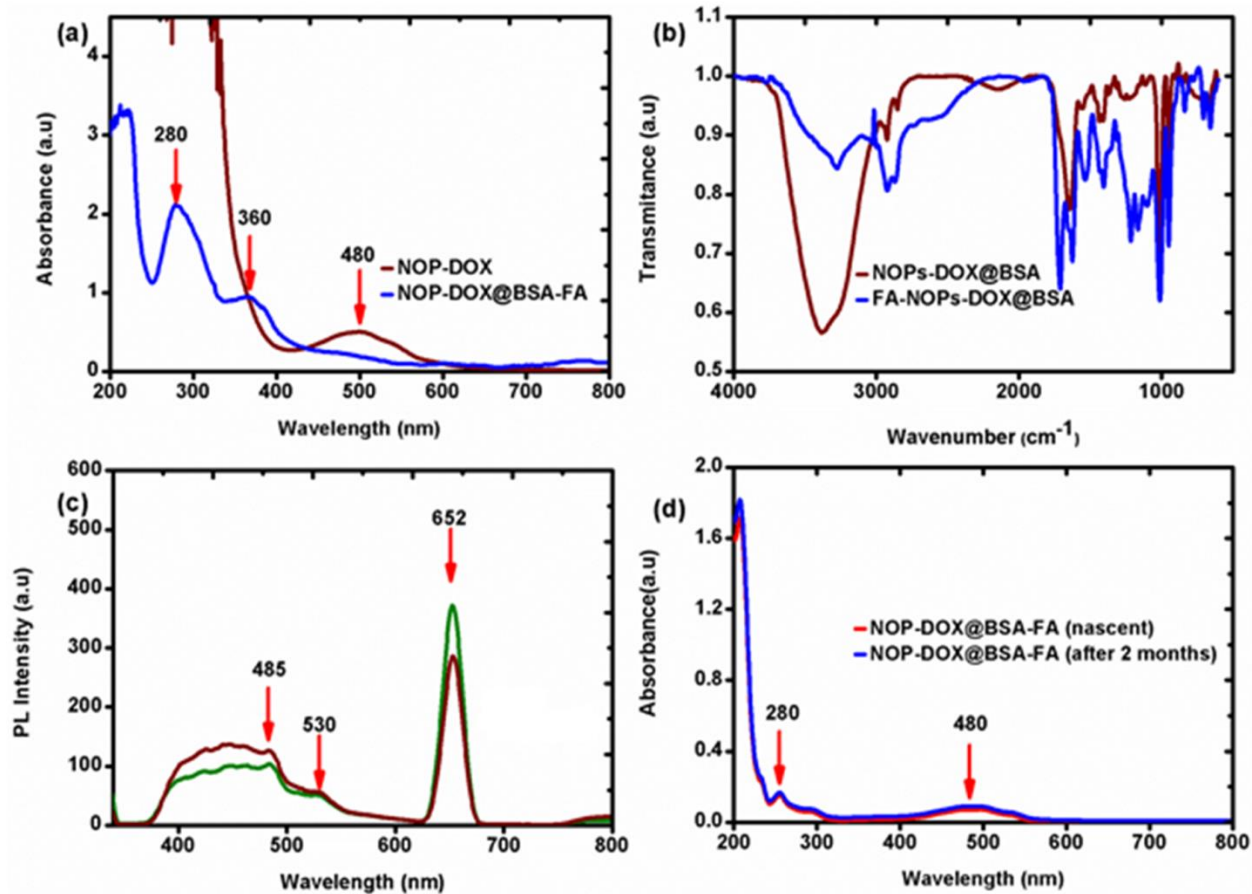


Figure S4 UV-Visible, FTIR and PL spectra of NOPs and its drug loaded conjugates.

(a) UV-Visible absorption spectra of NOP-DOX and NOP-DOX@BSA-FA. The maximum absorption wavelength of FA appeared around 280 nm, which is consistent with the absorption wavelength of NOP-DOX@BSA. (b) FT-IR spectra showing successful conjugation of FA onto NOP-DOX@BSA. (c) PL spectra of NOP-DOX and NOP-DOX@BSA show the emission peaks of lowest wavelength are observed at 404 nm and 423 nm, which correspond to the near-band emission (NBE) of NiO. The peaks at 423, 460, and 486 nm correspond to the blue emission, while the peak that arose at 527 nm represents green emission. The peak at 652 nm is a red emitting PL peak. (d)

UV-VIS spectra NOP-DOX@BSA-FA showing negligible decrease in absorption intensity after two months.

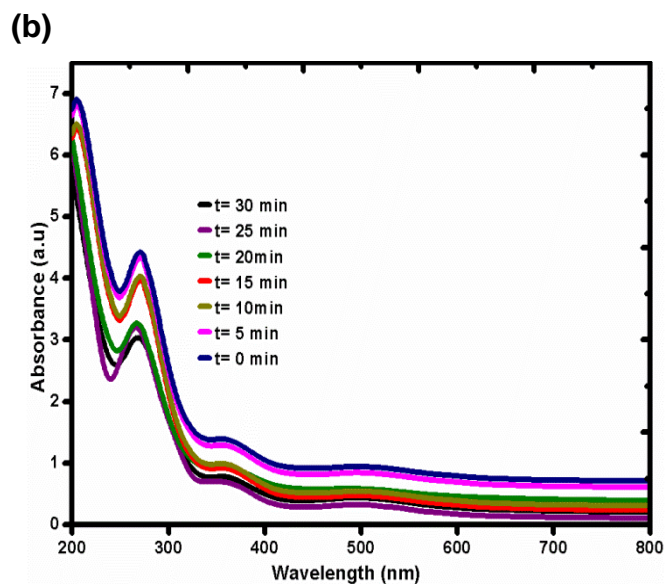
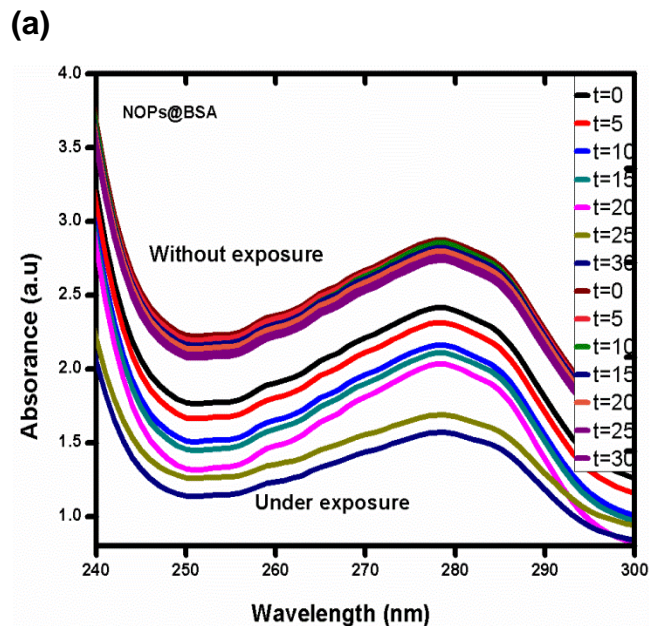


Figure S5 Effect of red light on absorption of BSA bound to NiO and drug release from NPs-DOX@BSA-FA. (a) The absorption intensity of BSA significantly decreased when irradiated in presence of NOPs. This shows that there could be a gross change in structural aspects. There was negligible shift in absorption maxima wavelength at different density of UV radiation. The change in absorption of BSA could be due to the minor structural and conformational changes in BSA. (b) A large decrease of absorbance around 270 nm (BSA and FA edge) was observed with approx.70% of change in 30 minutes

- [1] Zhou Z, Zhang C, Qian Q, Ma J, Huang P, Zhang X, et al. Folic acid-conjugated silica capped gold nanoclusters for targeted fluorescence/X-ray computed tomography imaging. *J Nanobiotechnology* 2013;11:17.
- [2] Ohkawa H, Ohishi N, Yagi K. Assay for lipid peroxides in animal tissues by thiobarbituric acid reaction. *Analytical Biochemistry* 1979;95:351-8.